Article

Characterization and 2D Self-Assembly of CdSe Quantum Dots at the Air–Water Interface

Kerim M. Gatts-Asfura, Celeste A. Constantine, Matthew J. Lynn, Daniel A. Thimann, Xiaojun Ji, and Roger M. Leblanc

J. Am. Chem. Soc., **2005**, 127 (42), 14640-14646• DOI: 10.1021/ja0514848 • Publication Date (Web): 04 October 2005

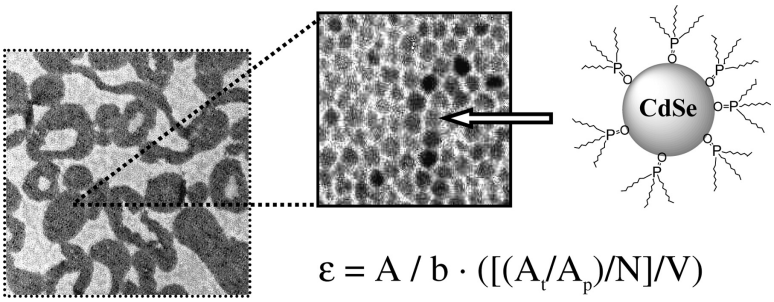

More About This Article

Additional resources and features associated with this article are available within the HTML version:

- Supporting Information
- Links to the 7 articles that cite this article, as of the time of this article download
- Access to high resolution figures
- Links to articles and content related to this article
- Copyright permission to reproduce figures and/or text from this article

View the Full Text HTML

J|A|C|S
ARTICLES
Published on Web 10/04/2005

Characterization and 2D Self-Assembly of CdSe Quantum Dots at the Air−Water Interface

Kerim M. Gattás-Asfura, Celeste A. Constantine, Matthew J. Lynn, Daniel A. Thimann, Xiaojun Ji, and Roger M. Leblanc*

Contribution from the Department of Chemistry, University of Miami, Coral Gables, Florida 33146

Received March 8, 2005; E-mail: rml@miami.edu

Abstract: Langmuir film properties, UV−vis spectroscopy, epifluorescence microscopy, and transmission electron microscopy were used to study CdSe quantum dots (QDs) in 2D. By combining these results, it was possible to determine the molar absorptivity, limiting nanoparticle area, luminescence property, and arrangement of the QDs in the monolayer films at the air−water interface. Either trioctylphosphine oxide (TOPO) or 1-octadecanethiol (ODT) stabilized the QDs. The data collected reveal that TOPO forms close-packed monolayers on the surface of the QDs and that ODT-stabilized QDs undergo alkyl chains interdigitation. It was also found that varying the nanoparticle size, nature of surfactant, surface pressure, and mixed monolayers could help engineer the 2D self-assembly of the QDs at the air−water interface. Of practical importance is the transfer of these monolayer films onto hydrophilic or hydrophobic solid substrates, which could be successfully accomplished via the Langmuir−Blodgett film deposition technique.

Introduction

Quantum dots-based nanostructures may be utilized as building blocks for photonic, electronic, and magnetic devices.[1−3] As a result, periodic arrays of semiconductor or other nanoparticles in all three dimensions are of current research interest. "Top-down" techniques (e.g., photo- and electron-beam lithography), several building supports including bioconjugation, and self-assemblies are being used to construct such nanostructures.[4−18] The self-assembly fabrication methods have shown great potentiality for directing the organization of nanoparticles.[19] This "bottom-up" methodology consists of inorganic/organic hybrid systems in which the nanoparticles assemble or co-assemble into superlattices.

Self-assembly of nanoparticles at the liquid−liquid[2] or air−water interface[20−27] has been investigated. Compressing QDs at the air−water interface could result in 2D monolayer films. Advantages of this assembly technique include establishing limiting nanoparticle area, easy manipulation of the films, and interparticle distance control. The latter is of great significance because much of the attention in quantum dots has been focused on their unique optical properties, which are sensitive to interparticle distance[28−30] and other factors, for example, particle size, material composition, nature of surface stabilizing molecules, and surrounding environment.

Langmuir films of QDs as a function of particle size[25,31] or nature of surface stabilizer[27] have been previously studied. However, a greater understanding of the QD monolayer proper-

(1) Nandhakumar, I. S.; Gabriel, T.; Li, X.; Attard, G. S.; Markham, M.; Smith, D. C.; Baumberg, J. J. *Chem. Commun.* **2004**, *12*, 1374.
(2) Lin, Y.; Skaff, H.; Emrick, T.; Dinsmore, A. D.; Russell, T. P. *Science* **2003**, *299*, 226.
(3) Guldi, D. M.; Zilbermann, I.; Anderson, G.; Kotov, N. A.; Tagmatarchis, N.; Prato, M. *J. Am. Chem. Soc.* **2004**, *126*, 14340.
(4) Huang, X.; Li, J.; Zhang, Y.; Mascarenhas, A. *J. Am. Chem. Soc.* **2003**, *125*, 7049.
(5) Liang, J.; Luo, H.; Beresford, R.; Xu, J. *Appl. Phys. Lett.* **2004**, *85*, 5974.
(6) Bachand, G. D.; Rivera, S. B.; Boal, A. K.; Gaudioso, J.; Liu, J.; Bunker, B. C. *Nano Lett.* **2004**, *4*, 817.
(7) Lee, J.; Govorov, A. O.; Dulka, J.; Kotov, N. A. *Nano Lett.* **2004**, *4*, 2323.
(8) Sheeney-Haj-Ichia, L.; Pogorelova, S.; Gofer, Y.; Willner, I. *Adv. Funct. Mater.* **2004**, *14*, 416.
(9) Gray, J. L.; Atha, S.; Hull, R.; Floro, J. A. *Nano Lett.* **2004**, *4*, 2447.
(10) Döllefeld, H.; Weller, H.; Eychmüller, A. *J. Phys. Chem. B* **2002**, *106*, 5604.
(11) Bäumle, M.; Stamou, D.; Segura, J.-M.; Hovius, R.; Vogel, H. *Langmuir* **2004**, *20*, 3828.
(12) Cui, Y.; Bjork, M. T.; Liddle, J. A.; Sonnichsen, C.; Boussert, B.; Alivisatos, A. P. *Nano Lett.* **2004**, *4*, 1093.
(13) Lu, N.; Chen, X.; Molenda, D.; Naber, A.; Fuchs, H.; Talapin, D. V.; Weller, H.; Müller, J.; Lupton, J. M.; Feldmann, J.; Rogach, A. L.; Chi, L. *Nano Lett.* **2004**, *4*, 885.
(14) Sashchiuk, A.; Amirav, L.; Bashouti, M.; Krueger, M.; Sivan, U.; Lifshitz, E. *Nano Lett.* **2004**, *4*, 159.
(15) Ravindran, S.; Bozhilov, K. N.; Ozkan, C. S. *Carbon* **2004**, *42*, 1537.
(16) Zhang, M.; Drechsler, M.; Müller, A. H. E. *Chem. Mater.* **2004**, *16*, 537.
(17) Lowman, G. M.; Nelson, S. L.; Graves, S. M.; Strouse, G. F.; Buratto, S. K. *Langmuir* **2004**, *20*, 2057.
(18) Cordero, S. R.; Carson, P. J.; Estabrook, R. A.; Strouse, G. F.; Buratto, S. K. *J. Phys. Chem. B* **2000**, *104*, 12137.
(19) Shenhar, R.; Rotello, V. M. *Acc. Chem. Res.* **2003**, *36*, 549.
(20) Selvakannan, P. R.; Swami, A.; Srisathiyanarayanan, D.; Shirude, P. S.; Pasricha, R.; Mandale, A. B.; Sastry, M. *Langmuir* **2004**, *20*, 7825.
(21) Yang, Y.; Pradhan, S.; Chen, S. *J. Am. Chem. Soc.* **2004**, *126*, 76.
(22) Achermann, M.; Petruska, M. A.; Crooker, S. A.; Klimov, V. I. *J. Phys. Chem. B* **2003**, *107*, 13782.
(23) Chen, S. *Langmuir* **2001**, *17*, 2878.
(24) Ferreira, P. M. S.; Timmons, A. B.; Neves, M. C.; Dynarowicz, P.; Trindade, T. *Thin Solid Films* **2001**, *389*, 272.
(25) Dabbousi, B. O.; Murray, C. B.; Rubner, M. F.; Bawendi, M. G. *Chem. Mater.* **1994**, *6*, 216.
(26) Huang, S.; Tsutsui, G.; Sakaue, H.; Shingubara, S.; Takahagi, T. *J. Vac. Sci. Technol., B* **2001**, *19*, 2045.
(27) Sui, G.; Orbulescu, J.; Ji, X.; Gattás-Asfura, K. M.; Leblanc, R. M.; Micic, M. *J. Cluster Sci.* **2003**, *14*, 123.
(28) Döllefeld, H.; Weller, H.; Eychmüller, A. *Nano Lett.* **2001**, *1*, 267.
(29) Kimura, J.; Uematsu, T.; Maenosono, S.; Yamaguchi, Y. *J. Phys. Chem. B* **2004**, *108*, 13258.
(30) Kotov, N. A.; Meldrum, F. C.; Fendler, J. H. *J. Phys. Chem.* **1994**, *98*, 8827.
(31) Kotov, N. A.; Meldrum, F. C.; Wu, C.; Fendler, J. H. *J. Phys. Chem.* **1994**, *98*, 2735.

10.1021/ja0514848 CCC: $30.25

ties as well as the 2D arrangement and luminescence properties of QDs in these systems is of broad interest.[17,27] Hence, the aims of this study were to characterize and manipulate the self-assembly of CdSe quantum dot monolayers at the air−water interface. The factors studied include particle size, nature of surfactant, surface pressure, and mixed monolayer systems. Characterization of the QDs or monolayer films was performed by UV−vis spectroscopy, surface pressure−area (π−A) isotherms, and transmission electron microscopy (TEM). Additionally, the luminescence properties of the QD Langmuir films together with the epifluorescence microscope were used to image the film topographies directly at the interface. Langmuir−Blodgett (LB) films of QDs on hydrophilic or hydrophobic solid substrates were also studied.

Experimental Section

Materials. Tetradecylphosphonic acid, 98% (TDPA), was acquired from Alfa Aesar (Ward Hill, MA). The water used was purified with a Modulab 2020 water purification system acquired from Continental Water Systems Corp. (San Antonio, TX). The purified water had a specific resistance of 18 MΩ cm, a surface tension of 72.6 mN/m at 20 ± 1 °C, and a pH of 5.7 ± 0.3. Oleic acid (*cis*-9-octadecenoic acid, >99%) was purchased from Calbiochem (San Diego, CA). All other chemicals and organic solvents were purchased from Sigma-Aldrich (St. Louis, MO) at the highest purity available. The chemicals were used as received.

Instrumentation. Surface pressure−area (π−A) isotherms were recorded on a Kibron Micro Trough S and Film Ware 2.41 software (Helsinki, Finland) at 19.0 ± 0.3 °C. Two computer-controlled movable barriers symmetrically regulated the surface area. The surface pressure was measured by the Wilhelmy method using a 0.51 mm diameter special alloy wire probe with a sensitivity of ±0.01 mN/m. The Langmuir trough with dimensions of 5.9 cm × 22.8 cm was equipped with a quartz window (located in the center of the trough) for in situ spectroscopic measurements or with a LB film deposition system. Langmuir−Blodgett films were deposited on quartz slides, which were cleaned and made hydrophilic using the well-known RCA procedures. When reacted with octadecyltrichlorosilane (0.4 g/L) in cyclohexane for 30 min, the slides became hydrophobic. These slides were purified by sonication and multiple rinsing cycles using cyclohexane.

An Olympus IX-FLA epifluorescence microscope (Melville, NY) was used for acquiring the epifluorescence images. UV light was used for excitation, and a thermoelectrically cooled Optronic Magnafire CCD camera detected the luminescence emission. The π−A isotherms and epifluorescence images of the QDs were collected within 2 days after preparation of the nanocrystals.

UV−vis absorption spectra were recorded on a Perkin-Elmer Lambda 900 UV/vis/NIR spectrometer (Norwalk, CT) using quartz cuvettes of 1 cm optical path length. Photoluminescence (PL) spectra were recorded on a Spex Fluorolog 1680 spectrometer (Edison, NJ). Elemental analysis was performed on a Philips/FEI XL-30FEG environmental scanning electron microscope (Hillsboro, Oregon) equipped with a field emission electron gun and a Link/Oxford X-ray analysis system for energy dispersive spectroscopy. The samples were prepared by drop coating silica plates followed by drying in air at room temperature. The LB monolayers were deposited on carbon-coated copper grids. One of the ends of a thin metallic wire was bent and utilized to clamp the copper grid, which was lifted up once through the air−water interface at a rate of 1 mm/min. Transmission electron micrographs of the QD or LB films were taken with a 80−100 kV Philips EM300 TEM equipped with eucentric goniometer stage, ±45° sample tilt.

Synthesis of TOPO-Capped CdSe QDs. The method followed for the synthesis of the QDs was reported by Peng and Peng.[32] The amounts of 0.0514 g of CdO, 0.2232 g of TDPA, and 3.7768 g of TOPO were loaded into a 25 mL flask with a condenser assembly and drying tube attached to it. The reaction mixture was heated to 310 °C under Ar flow and agitation. When a clear and colorless solution was obtained, the temperature was lowered to 270 °C followed by injection of 0.0411 g of Se powder dissolved in 2.4 mL of trioctylphosphine. Nucleation and growth of the QDs occurred at 250 °C until the desired particle size was reached. Immediately, the resulting solution was cooled to 60 °C and the QDs were collected and purified by precipitating/dispersing three times with 28 mL of anhydrous methanol/0.5 mL of chloroform. Further purification was achieved by washing the nanoparticles three times with a mixture consisting of 8 mL of anhydrous methanol and 2 mL of chloroform, followed by dispersion of the nanocrystals in 5 mL of chloroform and filtration through a 0.45 μm pore size polypropylene syringe filter, from Sigma-Aldrich.

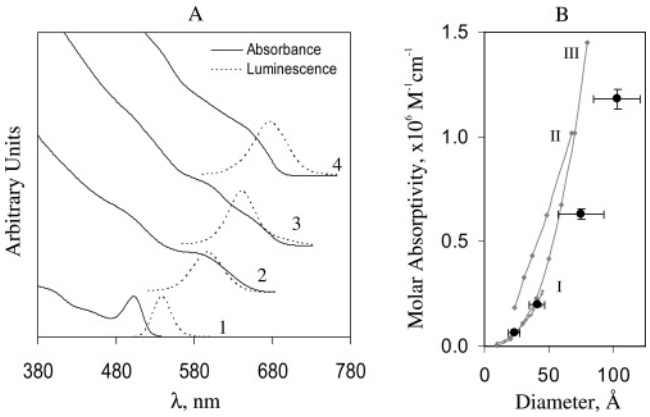

Figure 1. (A) Absorbance (solid lines) and PL (dashed lines, λ_{ex} = 400 nm) spectra of TOPO-capped CdSe QDs with average diameters of [1] 23 Å, [2] 41 Å, [3] 75 Å, and [4] 103 Å. (B) Molar absorptivity values of TOPO-capped CdSe QDs as a function of particle size. The error bars consist of the standard deviations for the respective axes. The dashed lines in (B) indicate the corresponding literature values. These data points were obtained from [I] Schmelz et al., Figure 1, ref 33; [II] Leatherdale et al., Figure 3, eq 7, ref 35; and [III] Yu et al., eq 6, refs 36, 37.

TOPO/ODT Surface Cap Exchange. To replace the TOPO surface cap on the CdSe QDs by an ODT cap, 1 mL of the TOPO-capped QDs in chloroform was reacted with 0.287 g (1 M) of ODT for ~19 h. The reaction mixture was kept under gentle agitation, in the dark, and at room temperature. Purification of the resulting ODT-capped CdSe QDs was achieved by first evaporating all of the chloroform present in the mixture utilizing argon flow. The QDs were then washed three times with 10 mL of the anhydrous methanol/chloroform (8:2, v/v) mixture. Finally, the QDs were dispersed in 1 mL of chloroform and filtered as described above.

Results and Discussion

Determination of molar absorptivity, limiting nanoparticle area, and the capacity to engineer the 2D organization of CdSe QDs in Langmuir films was investigated. Quantum dots of four different sizes were prepared, and TEM micrographs determined average diameters of 23, 41, 75, and 103 Å with standard deviations of 5 (22%), 6 (15%), 18 (24%), and 18 (18%), respectively. Adobe Photoshop 6.0 software was utilized to superimpose a circle onto each imaged particle (covering all of the dark area). The average size of the quantum dots was obtained by measuring the circle's diameter of 90 ± 60 particles according to the scale bar on the images. The absorbance and PL spectra of all four particle sizes are shown in Figure 1A. Because of the quantum confinement effects, both spectra red-shifted with increasing QD size.

(32) Peng, Z. A.; Peng, X. *J. Am. Chem. Soc.* **2001**, *123*, 183.

Molar Absorptivity of the QDs. The molar absorptivity (ϵ) of CdSe QDs at λ_{max} has been found to be dependent on nanoparticle size.[33−37] Linear,[35] cubic,[33,34] and intermediate between quadratic and cubic[36,37] functions are implied or reported in the literature as shown in Figure 1B. Molar absorptivity of QDs has been calculated from data collected by atomic absorption spectroscopy,[33,36−37] osmotic methods,[34] absorption cross section,[35] and/or controlled etching.[36,37] These literature ϵ values are included in the calculations to determine the concentration of QD samples prepared for this study.

In addition, it was found that UV−vis spectroscopy, surface pressure−area ($\pi-A$) isotherms, monolayer properties, QD size, and Langmuir−Blodgett (LB) films could be used collectively to determine the molar absorptivity of QDs. Proposed calculations and procedures are indicated in ref 38. Based on these combined results, the molar absorptivity values for the 23, 41, 75, and 103 Å CdSe QDs used in this study are 6.6×10^4, 2.0×10^5, 6.3×10^5, and 1.2×10^6 M^{-1} cm^{-1}, respectively. Although in close agreement with previously published calibration data, the derived ϵ values tend to follow a quadratic dependence (Figure 1B). This suggests that molar absorptivity is particle size-dependent and proportional to the QD surface area.

TOPO/ODT Surface Cap Exchange. The replacement of TOPO by ODT molecules on the surface of the QDs had a minimal effect ($\pm$ 1−3 nm) in λ_{max} of the nanocrystals' absorption and emission spectra. However, this surface cap exchange resulted in 86% quenching of PL intensity from the QDs. Introduction of S−Cd bonds on the surface of the CdSe QDs has been correlated to changes in PL properties arising from modifications of electronic states.[39−42] PL intensity was 98% quenched when an equimolar mixture of *N*,*N*-diisopropylethylamine (DIEA) and ODT was utilized to exchange the surface TOPO cap on the QDs. The nonnucleophilic base is utilized to facilitate binding of ODT to the QDs. However, utilization of DIEA during modification of the 103 Å QDs could result in a smaller average particle size, 79 Å, as imaged by the TEM. This suggests that chemical "etching" of the nanoparticles could take place with prolonged reaction time.

It has been proposed that every Cd atom on the surface of the CdSe QDs may be coordinated to a TOPO molecule.[43]

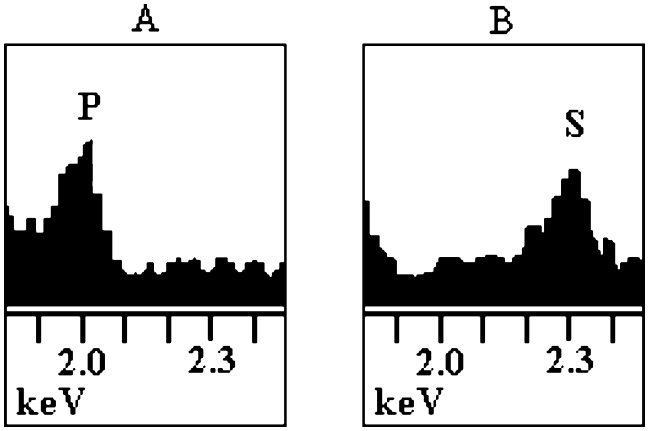

Figure 2. Energy-dispersive X-ray spectra of (A) TOPO-capped and (B) ODT-capped CdSe QDs. Intensity of *y*-axes = 3.00 k counts.

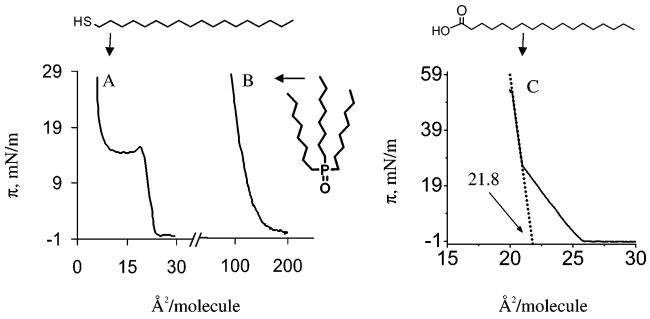

Figure 3. Characteristic $\pi-A$ isotherms for (A) ODT, (B) TOPO, and (C) stearic acid molecules.

Therefore, the degree of quenching of PL intensity could be correlated to the extent of surface ligand exchange. These changes in the QDs' optical properties provide evidence of an efficient surface cap exchange. To confirm these results, energy-dispersive X-ray analysis was performed on purified dried films of QDs. Appearance of a peak at 2.3 keV revealed the presence of sulfur atoms in the purified ODT-capped nanocrystals (Figure 2). The phosphorus peak at 2.0 keV decreased to the noise level of the spectrum. This indicates that ODT replaced most of the TOPO molecules on the surface of the QDs. The results compare to reports in the literature in which thiol-containing organic molecules could replace 85−90% of surface TOPO/TOPSe molecules on CdSe QDs.[42]

Limiting Nanoparticle Area. The limiting nanoparticle or limiting molecular area is defined as the smallest area occupied by the nanoparticle or molecule, respectively, in 2D. It is obtained by the extrapolation of the linear portion of the $\pi-A$ isotherm to zero surface pressure. First, the $\pi-A$ isotherms for the TOPO and ODT molecules were obtained. TOPO and ODT have limiting molecular areas of 135.0 and 22.5 Å^2/molecule, respectively, as shown in Figure 3A and B. ODT and stearic acid are very similar in structure, both having a C18 hydrocarbon chain but a different polar group. Both compounds have comparable limiting molecular areas of 22.5 and 21.8 Å^2/molecule, respectively (Figure 3A and C). No signs of ODT's thiol group oxidation were detected at the air−water interface (Supporting Information). The ODT $\pi-A$ isotherm has an additional feature. After the collapse of the monolayer film at about 15 mN/m, ODT presents a plateau region with almost

(33) Schmelz, O.; Mews, A.; Basché, T.; Herrmann, A.; Müllen, K. *Langmuir* **2001**, *17*, 2861.
(34) Striolo, A.; Ward, J.; Prausnitz, J. M.; Parak, W. J.; Zanchet, D.; Gerion, D.; Milliron, D.; Alivisatos, A. P. *J. Phys. Chem. B* **2002**, *106*, 5500.
(35) Leatherdale, C. A.; Woo, W.-K.; Mikulec, F. V.; Bawendi, M. G. *J. Phys. Chem. B* **2002**, *106*, 7619.
(36) Yu, W. W.; Qu, L.; Guo, W.; Peng, X. *Chem. Mater.* **2003**, *15*, 2854.
(37) Yu, W. W.; Qu, L.; Guo, W.; Peng, X. *Chem. Mater.* **2004**, *16*, 560.
(38) First, determine the UV−vis absorbance at the first excitonic peak (λ_{max}) of a QD solution (~0.19 mg/mL) in chloroform. Next, spread some (~85 μL) solution at the air−water interface on the Langmuir trough being sure π remains at 0 mN/m. Compress the film until a close-packed QD monolayer is reached (at $\pi \approx 35$ mN/m, solid monolayer phase of isotherm, and homogeneous topography as imaged by the epifluorescence microscope). Calculate concentration, *C*, in molarity of the solution in which $C = [(A_t/A_p)/N]/V$. A_t = the total area occupied by the QD monolayer on the trough. A_p = the average area occupied by a single QD in the monolayer. A_p is obtained by dividing a specific area of a TEM micrograph of the QD LB film by the number of QDs (closely packed) within this same area. Hence, A_p includes the interstitial space between QDs. *N* is Avogadro's number. *V* is the volume in L of the solution spread at the interface. Finally, the Beer−Lambert law is used to calculate ϵ of the QD.
(39) Seker, F.; Meeker, K.; Kuech, T. F.; Ellis, A. B. *Chem. Rev.* **2000**, *100*, 2505.
(40) Wuister, S. F.; de Mello Donegá, C.; Meijerink, A. *J. Phys. Chem. B* **2004**, *108*, 17393.
(41) Kalyuzhny, G.; Murray, R. W. *J. Phys. Chem. B* **2005**, *109*, 7012.
(42) Kuno, M.; Lee, J. K.; Dabbousi, B. O.; Mikulec, F. V.; Bawendi, M. G. *J. Chem. Phys.* **1997**, *106*, 9869.
(43) Taylor, J.; Kippeny, T.; Rosenthal, S. J. *J. Cluster Sci.* **2001**, *12*, 571.

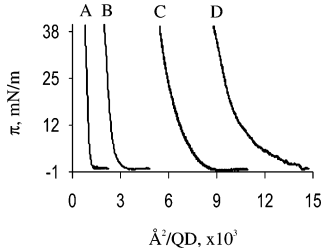

Figure 4. The $\pi-A$ isotherms of (A) 23 Å, (B) 41 Å, (C) 75 Å, and (D) 103 Å TOPO-capped CdSe QDs.

constant surface pressure followed by another rapid increase in surface pressure (Figure 3A). The limiting molecular area extrapolated from this second lifting point is 7.7 Å^2/molecule. This indicates the capacity of ODT to form a stable "multilayer" film at about 1/3 of its limiting molecular area. Self-assembly of ODT into a trilayer film has been reported on liquid mercury.[44]

The $\pi-A$ isotherms of QDs were recorded utilizing only fresh and purified QD samples. This practice was utilized to minimize the presence of 3D QD aggregates at the air−water interface. Considering a spherical nanocrystal, the area of a single TOPO-capped CdSe QD in 2D at the air−water interface could be predicted theoretically. Based on simple molecular modeling calculations, it has been reported that TOPO can form a monolayer on the surface of the nanocrystals.[43] Also, TOPO monolayers on metal surfaces have been measured at about 7 Å thick.[45] The area per QD in 2D then should be as follows: $\pi(r + 7)^2$, where r is the QD radius in Å. The QDs used in this study had average r values of 11.5, 20.5, 37.5, and 51.5 Å. The respective theoretical area/QD values in 2D are 1075, 2376, 6221, and 10 751 Å^2/QD. The corresponding experimental values of the limiting nanoparticle areas extrapolated from the $\pi-A$ isotherms (Figure 4) of the QDs are 1086, 2375, 6370, and 10 757 Å^2/QD, respectively. The predicted and experimentally derived limiting nanoparticle areas match very closely, with an error <3%. These results indicate minimum interdigitation of TOPO surface molecules, confirming that TOPO forms close-packed monolayers on the surface of the QDs. These results also prove the accuracy of the molar absorptivity values that were derived previously for the respective TOPO-capped CdSe QDs.

To verify that there is minimum interdigitation among the TOPO cap on the QDs, oleic acid was mixed with the 41 Å TOPO-capped nanoparticles at the QD molar fractions of 0.0, 0.1, 0.3, 0.5, 0.7, and 1.0. The respective $\pi-A$ isotherms of the solutions are shown in Figure 5A. The average area of the two-component films ($A_{1,2}$) obeyed the followed linear equation: $A_{1,2} = X_1(A_1 - A_2) + A_2$, where X_1 is the QD mol fraction, A_1 is the area (2003 Å^2) per pure QD at a π of 25 mN/m, and A_2 is the area (28 Å^2) per pure oleic acid at a π of 25 mN/m. A variation of <5% or R^2 value of 0.9938 for linearity was obtained (Figure 5B). The collapse pressure at >38 mN/m of the two-component films is characteristic of the QDs and does not vary much with composition. Therefore, it can be concluded that the two components of the mixed monolayer films are immiscible and that there is minimum interdigitation among the TOPO caps on the QDs or with oleic acid molecules.

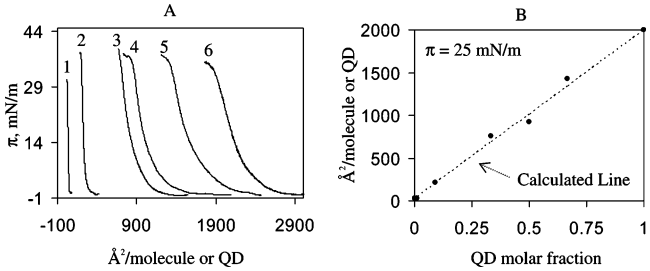

Figure 5. (A) The $\pi-A$ isotherms of the 41 Å TOPO-capped CdSe QDs and oleic acid mixed monolayers at the QD molar fractions of [1] 0.0, [2] 0.1, [3] 0.3, [4] 0.5, [5] 0.7, and [6] 1.0. (B) Comparison between the calculated [dashed line] and experimental [points] average areas of the respective two-component films at the different QD molar fractions.

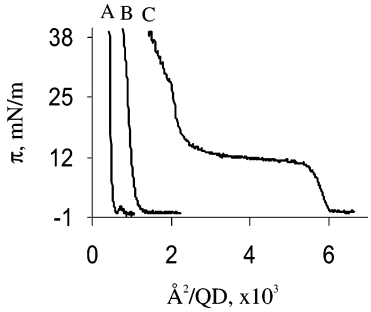

Figure 6. The $\pi-A$ isotherms of 23 Å CdSe QDs: (A) ODT-capped, (B) TOPO-capped, and (C) ODT-capped with 1:300 molar excess of free ODT.

The limiting nanoparticle area was lower for the ODT-capped QDs than for the corresponding TOPO-capped nanoparticles. For example, the 23 Å QD has a value of 505 or 1086 Å^2/QD when ODT- (Figure 6A) or TOPO-capped (Figure 6B), respectively. This suggests that replacement of the more bulky TOPO surface ligands with ODT molecules increases the packing density of the QDs through interdigitation of the longer ODT alkyl chains. However, this capacity for interdigitation facilitated 3D aggregate formation at the interface, which contributed to a smaller area/QD. This is explained in the next section devoted to the 2D self-assembly of the QDs.

The 23 Å ODT-capped CdSe QD solutions were "doped" with free ODT molecules at a 1:300 (QD:ODT) molar ratio. These free ODT molecules "dissolved" the QDs at the interface and reduced the formation of 3D aggregates; refer to the self-assembly section below. The $\pi-A$ isotherm of this mixed monolayer system is shown in Figure 6C, and its shape resembled that of the pure ODT monolayer (Figure 3). The limiting nanoparticle area extrapolated from the $\pi-A$ isotherm in Figure 6C is 6030 Å^2/QD. If there is no alkyl chain interdigitation, the area/QD after "doping" with ODT should have been [QD_{area} + (22.5 × 300)] or QD_{area} + 6750 Å^2/QD. In addition, the first collapse of the ODT monolayer film occurs at $\pi \approx 15$ mN/m, while that of the mixed monolayer with QDs occurs at $\pi \approx 10$ mN/m. This change in collapse surface pressure could be a result of miscibility and interdigitation of the two components at the interface.

The capacity of ODT to form a stable multilayer film at 1/3 its limiting molecular area was exploited to derive the limiting molecular area of a single 23 Å ODT-capped QD in the Langmuir film. The limiting nanoparticle area decreased from 6030 to 2474 Å^2/QD from the monolayer to the "trilayer" film (Figure 6C). If this decrease of 3556 Å^2/QD is divided by two, the area occupied by free ODT molecules in the "trilayer" mixed

(44) Kuzmenko, I.; Rapaport, H.; Kjaer, K.; Als-Nielsen, J.; Weissbuch, I.; Lahav, M.; Leiserowitz, L. *Chem. Rev.* **2001**, *101*, 1659.
(45) Jiang, J.; Krauss, T. D.; Brus, L. E. *J. Phys. Chem. B* **2000**, *104*, 11936.

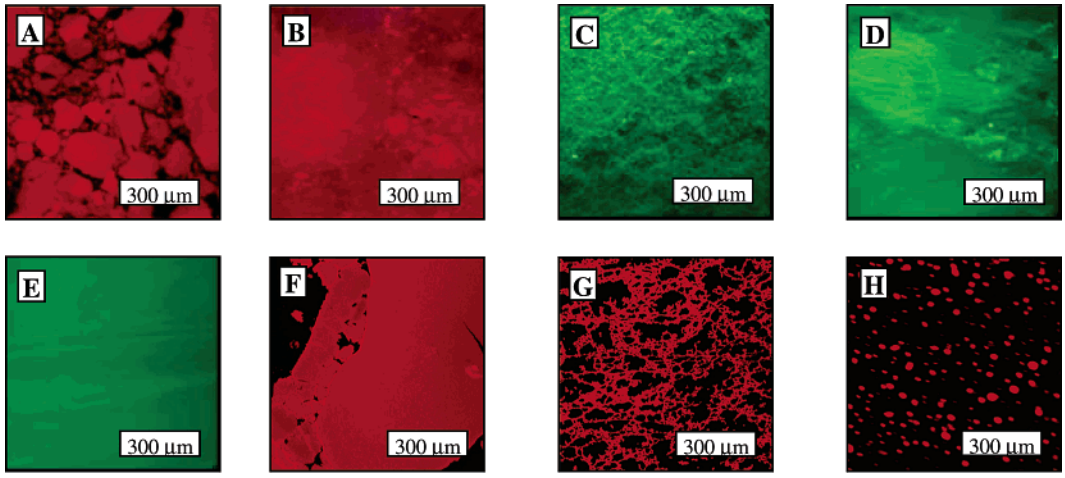

Figure 7. Epifluorescence images of the CdSe QDs taken directly at the air−water interface. (A) 103 Å TOPO-capped at 0 mN/m. (B) 103 Å TOPO-capped at 35 mN/ m. (C) 23 Å TOPO-capped at 39 mN/m. (D) 23 Å ODT-capped at 39 mN/m. (E) 23 Å ODT-capped + 300 molar excess free ODT at 35 mN/m. (F) 41 Å TOPO−CdSe at pH 10 and 50 mN/m. (G) 41 Å TOPO-capped mixed with oleic acid at a QD molar fraction of 1×10^{-3} at 25 mN/m. (H) 41 Å TOPO-capped mixed with oleic acid at a QD molar fraction of 1×10^{-4} at 25 mN/m. λ_{ex} = UV.

film is obtained, which is 1778 Å^2/molecule. Subtracting this value from the total 2474 Å^2/QD gives a limiting nanoparticle area of 696 Å^2/QD for the ODT-capped QDs. This new value indicates that the number of 3D aggregates was reduced and that still surface ODT's alkyl chains on the QDs interdigitated.

Similar studies and calculations were not performed for the larger ODT-capped nanoparticles. "Doping" these QDs with free ODT molecules at the same 1:300 molar ratio did not help to break all of the aggregates. This could be partially attributed to the larger particle size and changes in the degree of alkyl chain interdigitation. For example, the surface ODT molecules should have less free space (more crowded) as they extend away from the surface of larger nanoparticles. This was confirmed with the TEM micrographs taken for the 103 Å QDs as will be shown below.

Self-Assembly of the QDs in 2D. At zero surface pressure, the QDs self-assembled at the air−water interface into 2D domains as shown by the epifluorescence microscope (Figure 7A). Domain formation was more obvious as particle size increased. Upon compression, the domains organized into a more uniform film at a surface pressure of about 35 mN/m (Figure 7B). The nature of the surface cap on the QDs can also influence interparticle interactions and topography at the air−water interface. For example, the 23 Å TOPO-capped CdSe QDs presented a corrugated topography at the high surface pressure of 39 mN/m (Figure 7C). The film collapsed with further increase in surface pressure. This particular topography was not observed for the ODT-capped QDs of the same size even at higher surface pressures (Figure 7D).

The addition of 300 molar excess of free ODT molecules in solution "dissolved" the 23 Å ODT-capped QDs, which then presented more homogeneous topographies as shown in Figure 7E. "Doping" the solutions of the larger ODT-capped QDs with free ODT molecules at the same molar ratio did not result in homogeneous films as above. Brighter domains were still visible at the air−water interface. Multilayer domains or 3D aggregates may contribute to the appearance of these brighter areas as a consequence of QD photoluminescence changes at the interface. For example, PL intensity of the QD Langmuir films was enhanced or underwent photochromism from red to green upon UV irradiation over time, as observed with the epifluorescence microscope. These changes in PL properties of the QDs may result from photooxidation of the nanocrystal surface or cap.[46,47] In addition, water molecules decreased the photoluminescence intensity of the TOPO-capped CdSe QDs. The effect of water molecules on the PL intensity of QDs in Langmuir films has been reported previously.[18] When the monolayer film was transferred to a quartz slide via the LB film deposition method, the PL from the QDs was easily detected on the dried film. However, an optical fiber attached to the spectrofluorimeter did not detect any PL emission from the CdSe QD monolayer when positioned directly above it at the air−water interface. This was a result of low PL intensity.

Some of the nanoparticles within 3D aggregates could be oriented more into the air and further away from the water molecules. This could result in a higher PL intensity in addition to the increased concentration of nanoparticles in these 3D domains. It is known that aggregation or high concentrations of QDs and fluorophores in general may result in lower or quenching of PL intensity of solutions because of inner filter effects, radiative and nonradiative transfer, excimer formation, or other. For example, the 23 Å TOPO-capped QD chloroform solutions decreased (6−75%) PL intensity and red-shifted (>10 nm) emission λ_{max} when the concentration level was increased from 7×10^{-6} to 30×10^{-6} M. However, it was assumed that photooxidation, interparticle interactions, or 3D self-assembly of the QDs at the interface enhanced PL intensity, and the aggregates appeared brighter. To support this assumption, QDs were spread onto a glycerol or basic (pH 10) subphase. The QDs had difficulties spreading through the interface and formed multilayer domains as illustrated in Figure 7F. These domains were brighter when imaged with the epifluorescence microscope, and their PL emission was detected with the optical fiber device.

To further manipulate the 2D self-assembly of QDs at the air−water interface, mixed monolayer systems were also studied. The 41 Å TOPO-capped QDs were mixed with oleic acid at different molar fractions. Oleic acid was used because it should not replace the TOPO surface molecules on the QDs and may impart some organizational features because of its single double bond (18:1, *cis*-9). At the QD molar fraction of 1×10^{-3}, the

(46) Aldana, J.; Wang, Y. A.; Peng, X. *J. Am. Chem. Soc.* **2001**, *123*, 8844.
(47) Myung, N.; Bae, Y.; Bard, A. J. *Nano Lett.* **2003**, *3*, 747.

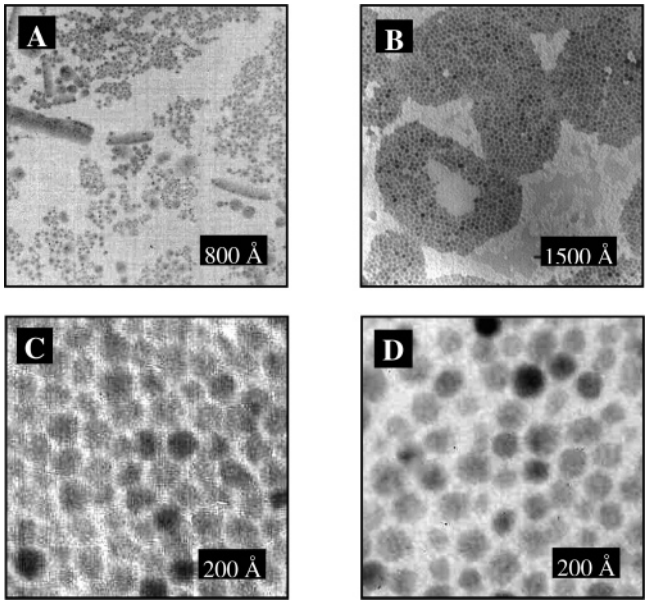

Figure 8. TEM micrographs of CdSe QD LB monolayer films deposited on carbon-coated copper grids at 20 mN/m. (A) 75 Å TOPO-capped. (B) 103 Å TOPO-capped. (C) 103 Å TOPO-capped. (D) 103 Å ODT-capped.

2D domains formed a totally new topography as shown in Figure 7G. The QDs self-assembled into domains, which formed a 2D structure such as those found in porous materials. At the lower QD molar fraction of 1×10^{-4}, separate domains between 10 and 41 μm in size were imaged as shown in Figure 7H.

These QD micro-domains moved collectively across the monolayer film even at high surface pressures. The conditions for imaging the topography were adjusted so that the images show the real domains as seen with the naked eye through the epifluorescence microscope. The actual color of the domains may have varied slightly as a result. This observed "fluidity" of the mixed monolayer may be a result of the cis double bond on oleic acid. Unsaturated fatty acids have kinks and do not pack as well as saturated fatty acids. Therefore, an increase in the composition of unsaturated fatty acids results in increased lateral fluidity on a membrane or unstable/"fluid" monolayer film. When stearic acid, a saturated fatty acid, instead of oleic acid was utilized to prepare the mixed monolayer films, static topographies were barely imaged. PL intensity was almost completely quenched. Imaging of the topography was difficult at the low QD molar fractions, which were needed to evaluate QD "fluidity" within the film.

Besides surface alkyl chain interdigitation and the closest possible packing arrangement of QDs, the degree of organization at the air−water interface may also be influenced by other factors. For example, surfactants such as TOPO and the crystalline structure of the CdSe nanoparticles could bring about intrinsic dipole moments.[43,44] Changes in surface cap and nanocrystal size may alter the direction and intensity of these polarities, which may be factors influencing the degree of nanoparticles organization at the interface.

To study the organization of the QDs at the air−water interface, TEM micrographs of LB monolayer films were taken at the π of 20 mN/m. The QDs self-assembled into domains of variable architecture as shown in Figure 8A,B. The nanoparticle organization within the 2D domains was influenced by the nature of the surface stabilizing molecule. TOPO-capped QDs had

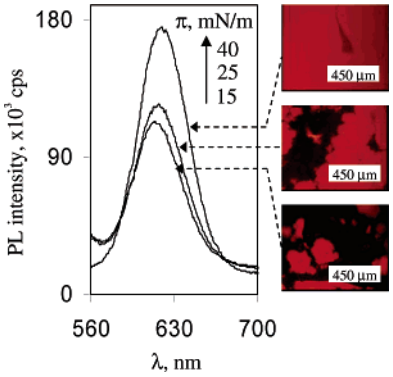

Figure 9. PL spectra and epifluorescence images (λ_{ex} = UV) of a 41 Å TOPO-capped CdSe QD LB monolayer film deposited on a hydrophilic quartz slide at different surface pressures.

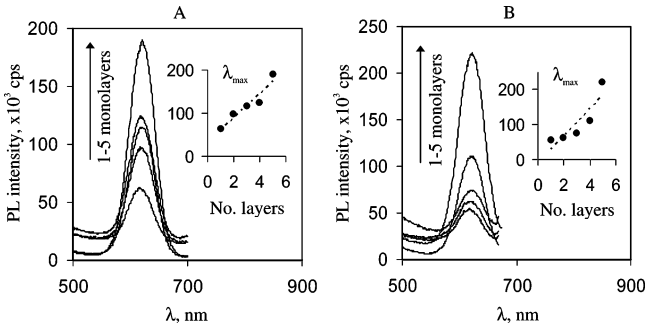

Figure 10. Increase in PL intensity of 41 Å TOPO-capped CdSe QDs LB films on (A) hydrophilic and (B) hydrophobic quartz slides as a function of the number of deposited monolayers. Deposition π of 25 mN/m and λ_{ex} of 467 nm.

hexagonal like close-packing arrangements as shown in Figure 8C. Deviations from the hexagonal packing of QDs could be attributed in part to the large particle size distribution of the samples. The ODT-capped nanocrystals were found to have areas in which the QDs were farther apart from each other (Figure 8D). A longer interparticle distance confirmed the presence of the longer ODT on the surface of the nanoparticles. Interdigitation was then more restricted at this large particle size. Some 3D domains within the LB films were detected as darker or indistinct areas.

Manipulation of the QD Langmuir Films. QD Langmuir films were transferred onto hydrophilic or hydrophobic quartz slides utilizing the LB film deposition technique at different surface pressures. Deposition ratios higher than 0.8 were obtained for both substrates indicating an effective film transfer. Emission from a single TOPO-capped QD LB monolayer film was detected. When deposited at higher surface pressures, the LB monolayer increased PL intensity (Figure 9). This results from a closer packing of the QD domains as shown in Figure 9. When imaged with the epifluorescence microscope, the topography of the QD LB films deposited at different surface pressures on the slides resembled that taken directly at the interface. Thus, the films were transferred nearly intact as assembled at the air−water interface.

Photoluminescence intensity from the LB films on the hydrophilic quartz slide increased linearly ($R^2 = 0.9115$) with the number of QD monolayers (Figure 10A). This suggested that equal amounts of QDs were transferred after each deposition cycle, which resulted in a buildup of a homogeneous film. TOPO-capped QD deposited on the hydrophobic quartz substrate

had a lower correlation coefficient for linearity, $R^2 = 0.7748$ (Figure 10B). However, the total PL intensity from the hydrophilic or hydrophobic LB films was within the same range after deposition of the 5 QD monolayers. Therefore, deviations from linearity could be partially attributed to variations in the deposition ratio, the distribution of the QD domains along the solid support, and the area in which PL intensity was recorded. The stability of the films was not evaluated herein.

Conclusions

Langmuir films were utilized to determine the molar absorptivity of CdSe QDs and to study the capacity for manipulating the 2D organization of the QDs. Surface modification, particle size, surface pressure, and mixed monolayer systems all influenced the self-assembly of the QDs at the air−water interface. Stoichiometry within the mixed monolayer systems also directed the self-assembly of QDs in Langmuir films. The QDs monolayers were readily transferred onto solid substrates via the LB film deposition technique. Controlling nanoparticle organization and transferring the nanostructured films to the desired substrate could enhance the application of QDs in optoelectronic or magnetic devices, including those for chemo- and biosensing. It is known that QDs may aggregate over time. This should result in a decrease of the limiting nanoparticle area extrapolated from the $\pi-A$ isotherms. Therefore, the Langmuir film may be utilized additionally as a tool to monitor time-related stability of QDs.

Acknowledgment. This work was supported by the National Science Foundation (CHE-0416095).

Supporting Information Available: Stability of the ODT's thiol group against oxidation at the air−water interface. This material is available free of charge via the Internet at http://pubs.acs.org.

JA0514848